

HADES - A HIGH ACCEPTANCE DIELECTRON SPECTROMETER PROPOSED FOR RELATIVISTIC HEAVY-ION COLLISIONS¹

H. Neumann², A. Borsche², K. Garrow, H. Bokemeyer, W. Koenig,
F. Lefèvre, P. Salabura, R. Schicker, A. Schröder, J. Stroth
GSI, 64220 Darmstadt, Germany
for the HADES COLLABORATION³

Received 5 April 1994, accepted 2 May 1994

A High Acceptance Dielectron Spectrometer (HADES) has been proposed at the SIS accelerator of GSI in order to measure e^+e^- pairs produced in central nucleus-nucleus collisions. HADES will be able to operate at the highest luminosities available at SIS in an environment of high hadron and photon background. A Ring Imaging Čerenkov Counter (RICH) serves for electron identification. Momentum measurement is achieved with a magnetic spectrometer consisting of superconducting toroidal coils and mini drift chambers for tracking. Arrays of shower detectors and scintillator paddles are positioned behind the drift chambers for electron trigger purposes and for measuring the charged particle multiplicity. The detector features have been investigated in detailed simulations. Results for the expected dielectron yield and the combinatorial background are presented as a function of the pair mass.

1. Introduction

Heavy-ion collisions in the energy domain of SIS or AGS offer a unique possibility to investigate the properties of hot, compressed nuclear matter. The goal is to derive the nuclear equation of state (EOS). At bombarding energies of about 1-2 GeV/nucleon, baryon densities of 2-3 ρ_0 and temperatures up to 100 MeV can be reached during the collision phase. Here, ρ_0 denotes the nuclear ground state density of 0.17/fm³. Due to the high density of this phase new particles are produced in multiple baryon-baryon collisions.

¹Presented by H. Neumann at School and Workshop on Heavy Ion Collisions, Bratislava, 13-18 September 1993

²E-mail address: hneumann@vscn.gsi.de

³IOF Bratislava, Univ. Clermont-Ferrand, GSI Darmstadt, Univ. Frankfurt, Univ. Gießen, Univ. Krakow, ITEP Moscow, LPI Moscow, MEPI Moscow, TU München, Univ. Nikosia, INP Rež, Univ. Valencia

Electromagnetic probes like virtual photons decaying into electron-positron pairs play a special role in this context. In contrast to hadrons they carry away information about the hot, compressed phase undistorted by strong final state interaction. In the SIS energy regime the dominant dilepton-production mechanisms are Dalitz-decays ($X \rightarrow N e^+ e^-$, $X \rightarrow \gamma e^+ e^-$) and two body decays ($X \rightarrow e^+ e^-$) of hadrons as well as nucleon-nucleon bremsstrahlung. Dielectrons originate from the compressed phase if the time scale of the corresponding production processes is on the order of the duration of the high density phase of about 10 fm/c. This is the case for nucleon-nucleon bremsstrahlung and for the Δ and ρ resonances with life times of the free particles of about 1.5 fm/c. The Dalitz decays of η and π^0 occur outside the dense phase due to the long life times. Since η and π^0 suffer absorption and subsequent reemission in the expansion phase their dielectrons carry no direct density information. They contribute to the dilepton mass spectrum up to their rest mass of 135 MeV/c² and 549 MeV/c², respectively. For heavy systems such as Au+Au the spectrum below 500 MeV/c² is dominated by η , with additional contributions from pn-bremsstrahlung and Δ decay. Above 500 MeV/c² dominant contributions from the two body decays of the vector mesons $\rho(770 \text{ MeV}/c^2)$, $\omega(783 \text{ MeV}/c^2)$ and $\phi(1020 \text{ MeV}/c^2)$ are expected [1][2][3].

The two body decays of the vector mesons are of special interest since width and mass of the resonances are accessible in dilepton mass spectra. While the large width of the ρ results in a broad $e^+ e^-$ mass distribution, ω and ϕ are more easily identified due to their narrow widths. Since these widths correspond to larger life times only a small fraction of dielectrons will be produced by ω and ϕ decay at high densities. However, one expects that the rapidity and transverse-momentum distributions for vector meson decay in the hot phase differ from the decay in the expansion phase. This offers an experimental access to the hot, dense phase by selecting high dielectron energies.

Vector meson properties, i.e. mass and width are expected to be strongly modified in a dense and hot hadronic environment. Boson exchange models [2][4][5] anticipate an increase of the resonance width with density, while the mass is predicted not to change. In contrast, results from QCD inspired calculations [6][7] predict significant mass shifts with increasing density. These medium modifications should lead to significant effects in the experimentally observed dilepton spectrum [1][2][8].

2. Experimental Considerations

Due to the weak electromagnetic coupling the dilepton decay channel of vector mesons is suppressed by a factor of $\approx 10^{-5}$ as compared to the hadronic decay channel. Together with the small subthreshold production cross sections the total yield of dielectrons from vector mesons is only of the order of 10^{-6} per central Au+Au collision at 1 AGeV [9]. Thus the experimental challenge is to find one dilepton in one million of these central collisions each containing about 400 hadrons and 25 photons from π^0 -decay. For a light system such as Ca+Ca at 1 AGeV the dilepton cross section is even smaller by a factor of about 25.

Dilepton production in the SIS/Bevalac energy regime has been pioneered by the DLS collaboration at the Bevalac in Berkeley [10][11]. The two arm spectrometer DLS

uses large aperture dipole magnets together with drift chambers for momentum measurement and gas threshold Čerenkov counters in front and behind for redundant electron identification.

For light systems (p+p, p+d, p+Be) the DLS measurements led to an identification of the basic processes of dilepton production in this energy regime. Moreover, an indication of the vector meson contribution to these dilepton mass spectra was found.

The heaviest systems measured with DLS were heavy ion reactions of Ca+Ca and Nb+Nb. Within the current statistics of these data, a clear vector-meson signal can not be established. Due to the high hadron multiplicity DLS could not handle heavier systems such as Au+Au. However, the dilepton production rate in this heavy system is more than an order of magnitude larger than in the Ca+Ca system resulting in higher dilepton statistics per measuring period. Moreover, the mass resolution of the DLS spectrometer in the $p/\omega/\phi$ region is not sufficient to resolve ω ($\Gamma_{free} = 8.5 \text{ MeV}/c^2$) and ϕ ($\Gamma_{free} = 4.4 \text{ MeV}/c^2$) from the ρ distribution ($\Gamma_{free} = 150 \text{ MeV}/c^2$). Therefore, a new detector HADES has been proposed to study in-medium modifications of vector mesons [12][13].

3. Design of the Spectrometer

Studying small dilepton production probabilities of the order of 10^{-6} per central collision requires maximum acceptance over the whole kinematical range and the ability of operating at high luminosities (10⁶ collisions/s). In the presence of a strong hadronic background excellent background rejection capabilities are required. The proposed device is a rotationally symmetric, large acceptance spectrometer oriented along the beam axis. With this geometry complete azimuthal coverage is achieved. The design values for the angular and momentum acceptance were chosen according to the two body decay kinematics at SIS energies assuming thermal emission from a midrapidity zone. These dielectrons are emitted over the whole polar angular range with a maximum intensity at about 40°. HADES will cover polar angles from 18° to 85°. For masses up to 1.5 GeV/c² and transverse momenta up to 1.5 GeV/c this geometry results in a flat acceptance. The efficiency of $\sim 40\%$ represents an improvement by a factor of 100 as compared to the DLS.

The proposed strategy for the measurement of dielectrons - (1) electron identification, (2) momentum determination, (3) electron trigger - is similar to the DLS but the HADES concept fulfills the requirements of a large acceptance spectrometer (Fig. 1.):

1. Individual electron identification over the full acceptance is done by a RICH (ring imaging Čerenkov counter) with gas radiator surrounding the target in the forward hemisphere.
2. Momentum analysis is achieved by trajectory reconstruction in the magnetic field section. A toroidal field geometry (6 coils) is the optimal choice for the following reasons: First, while covering the large forward solid angle, a field free region for the RICH can be accommodated inside the toroid. This ensures undisturbed Čerenkov rings. Second, the field geometry is well matched to the dilepton

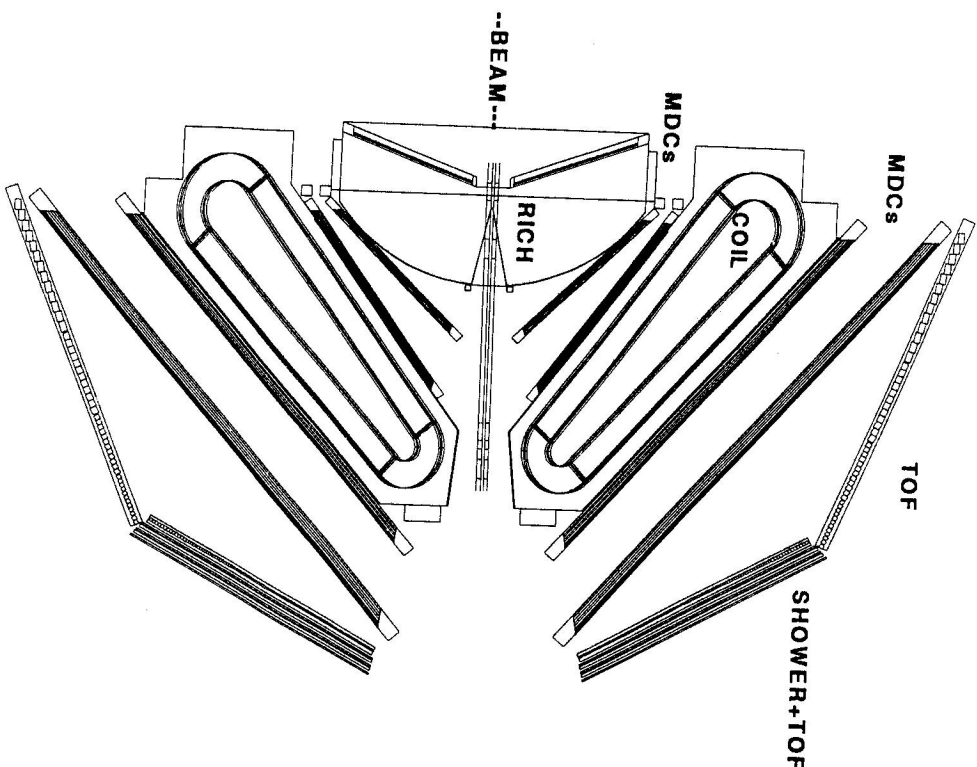


Fig. 1. Azimuthal cross section of the HADES setup. The RICH consists of radiator gas, carbon fiber mirror and the tilted UV detector segments. The target is positioned in the center of the radiator. Two sets of mini-drift chambers (MDCs) in front and behind the magnetic field produced by superconducting coils measure the trajectory. A time of flight wall (TOF) is foreseen as a first level trigger and for second electron identification. At polar angles $< 45^\circ$ electron identification is achieved with a shower detector in combination with the TOF wall.

kinematics since the radial $1/r$ dependence of the field compensates for the fact that the mean momentum increases for decreasing polar angles. The coils are superconducting and iron-free in order to minimize the size of the spectrometer and to reduce secondary background. Mini-drift chambers (MDCs) are positioned in front and behind the field region for tracking purposes.

3. As a first level trigger on central events and for fast electron triggering META (Multiplicity and Electron Trigger Array), a scintillator wall combined with a shower detector, surrounds the outer MDCs.

The performance of the spectrometer was studied by detailed simulations using GEANT and including the complete geometry of the setup as well as realistic detector responses. A 3-dimensional magnetic field map based on the toroidal coil geometry was used for tracking. As a worst case scenario 1 AGeV central Au+Au collisions were investigated.

4. The RICH Detector

The RICH is the main component for electron identification. It consists of a gas radiator surrounding the target in the forward hemisphere (Fig. 2.). The Čerenkov light from electrons emitted in a cone is reflected by a spherical carbon fiber mirror (radius 90 cm, thickness 0.2 cm) and focused onto a position sensitive UV detector.

The UV detector is a MWPC with a solid photocathode of evaporated CsI. It is separated from the radiator volume by a 8 mm CaF_2 window. The solid photocathode is divided into square pads of 6 mm and has a distance of 1mm to the anode wires. The average quantum efficiency increases with shorter wavelengths and reaches 45% at the radiator transmission cutoff of 140 nm. The expected single photoelectron detection efficiency is about 90%. Each of the 5800 pads per sector will be read out separately.

The ring quality is mainly determined by the focusing properties of the mirror due to an extended and curved focusing area (spherical aberration) (Fig. 2.). For large lepton emission angles the focal points for parallel Čerenkov rays propagating in the plane shown or in a perpendicular plane (azimuthal) differ significantly. This results in elliptically deformed ring images. The 20° tilt angle of the six azimuthal UV detector segments is matched to this focal area.

A radiator gas mixture of 50% C_4F_{10} and 50% CH_4 is proposed for the following reasons:

1. The threshold value $\gamma_{th} \approx 22$ yields a sufficient number of Čerenkov photons. Nevertheless, hadron blindness for the given momentum range is achieved. All protons and practically all pions have velocities below the radiator threshold ($p_{th}^p \approx 20 \text{ GeV}/c$, $p_{th}^\pi \approx 3.1 \text{ GeV}/c$). For electrons the threshold amounts to $p_{th}^e \approx 11.1 \text{ MeV}/c$ which is well below the HADES momentum range.
2. The high UV transmission with a cutoff below 145 nm results in a high Čerenkov photon yield per unit path length. The radiator can therefore be built in a compact way.
3. From scintillation light measurements for C_4F_{10} and CH_4 [13] only a small number of scintillation photo electrons of ≤ 30 /collision is estimated (single hits in Fig. 3.).
4. The choice of this gas mixture compared to pure C_4F_{10} has the advantage of a reduction of the radiation length by a factor of 2 while the photon yield is only reduced by 30%. This results in a smaller amount of external pair conversion (EPC) of γ rays from high energy π^0 .

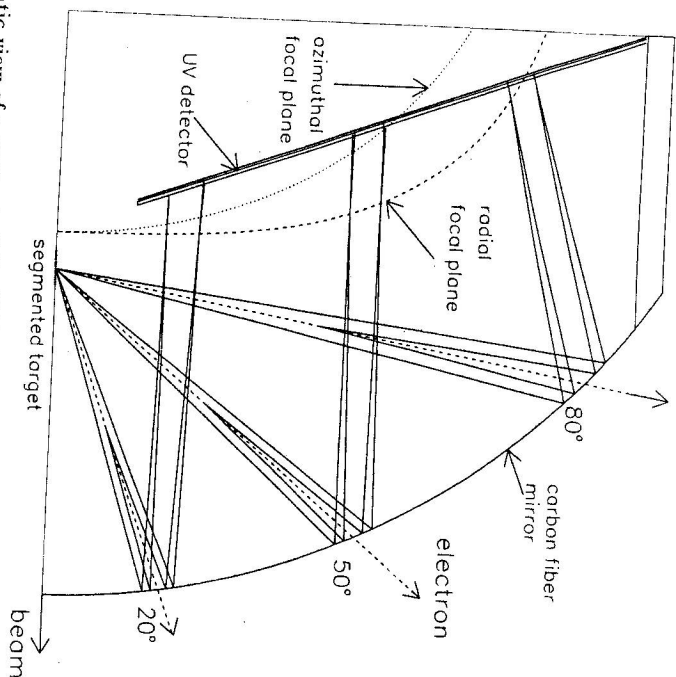


Fig. 2. Schematic view of a segment of the HADES Ring Imaging Čerenkov Counter (RICH): Electrons passing the radiator produce Čerenkov photons, which are reflected by the carbon fiber mirror and focused towards the UV detector. The (radial) focal plane for parallel rays in the plane shown is given by the dashed curve. The dotted curve shows the azimuthal focal plane for Čerenkov photons emitted perpendicular to this plane. Tilt angle and position of the UV detector are adapted to the shape of the focal area

Within the range of lepton emission angles θ , corresponding to radiator lengths of 42-73 cm, 15-26 photons are detected per ring. These numbers have been calculated for the given detection efficiency of the UV-detector including transmission losses in the radiator gas and the CaF_2 window and losses due to the mirror reflectivity (0.85).

Most of the Čerenkov rings are due to the π^0 decay products. EPC in the segmented target and in the radiator contributes equally with $\sim 0.2/\text{collision}$. Only one ring is produced by such pairs due to the small mean pair opening angle of $\sim 0.5^\circ$. The Dalitz pairs (0.13 pairs/collision) have a larger mean opening angle of $\sim 0.5^\circ$. The Dalitz overlapping rings. After rejecting pairs of rings with opening angles smaller than 15° the number of single background rings amounts to $\sim 0.5/\text{central collision}$. Further rejection methods have to be applied (see below) since combinatorial background from Dalitz and EPC pairs results in an opening angle distribution similar to that of the two body decay (mean opening angle 90°).

Fig. 3. shows a typical RICH hit pattern as a simulation result for 1 AGeV Au+Au collisions. The two Čerenkov rings marked by circles are produced by an ω decay contained in this event.

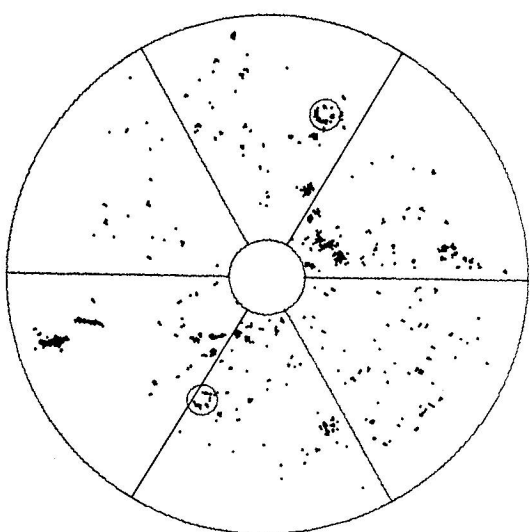


Fig. 3. RICH hit pattern for 1 AGeV Au+Au collisions containing one e^+e^- pair from ω . The Čerenkov rings produced by the electrons are marked with circles. The clusters originate from ionisation of charged particles and from Čerenkov light produced in the CaF_2 window. Single hits are due to scintillation light and electronic noise.

The first step of the RICH analysis is a transformation of the elliptical images into circles. Afterwards, a two step ring to center transformation allows an efficient identification of circles in the presence of background. The rings are subsequently fitted by a least squares procedure. The track angle is calculated from the ring center. The efficiency to detect and reconstruct rings from e^+e^- pairs of ω amounts to 95%.

5. The Magnetic Spectrometer

The required momentum range covers ~ 200 MeV/c to ~ 1.5 GeV/c. For the two body decay at beam energies of 1-2 AGeV the mean electron momentum varies from 800 MeV/c at a polar angle of 20° to 300 MeV/c at 85° . A mass resolution of the order of the ω -width requires a momentum resolution of $\Delta p/p \leq 1.5\%$ (σ). This specification can be obtained with a momentum kick of 50 to 100 MeV/c and a spatial resolution of each module of ≤ 100 μm (σ) for the geometry chosen.

The toroidally shaped magnetic field ($B_{max} = 3.8$ T) will be generated by 6 superconducting coils with individual but interconnected vacuum vessels. A slim construction of each coil unit minimizes solid angle losses. A low-mass design and use of low-Z materials is necessary to minimize secondary particle production.

Tracking is done outside of the torus with mini-drift chambers, two before and two after the magnetic field region. In order to minimize multiple scattering the volumes in between the MDCs - in particular the magnetic field region - are filled with Helium.

The unambiguous reconstruction of tracks by the drift chambers is demanding due to the large primary charged particle multiplicity per collision. The multiplicity measured along the polar coordinate and integrated over the perpendicular direction within one sector amounts to a maximum of 0.6/cm in the innermost MDC. In the outer MDCs the hit density reaches values of 0.22/cm. In this number, an amount of 15% secondaries produced in the coils and in the inner detectors is included. To handle this high multiplicity, each module consists of 6 wire planes with a small sense wire spacing ranging from 5 mm in the innermost detector to 14 mm in the outermost detector. With this wire spacing a double hit probability of less than 0.3 per wire is achieved. The wire tilt angles in the 6 MDC planes vary from -40° to $+40^\circ$ in 20° steps. The wire positions of the 3rd and 4th plane with 0° tilt angle differ by half a pitch. The choice of these tilt angles ensures an optimal polar angle resolution which is most relevant for a good momentum resolution.

For the reconstructed hitpoints the momentum vector and the vertex of the trajectory are obtained by a global fit. The resulting invariant mass resolution in the ρ/ω meson (Fig. 5b). For the given field the resolution at large momenta is limited by the spatial resolution of the tracking detectors whereas at low momenta it is limited by multiple scattering in the field region. The mass resolution is improved by more than an order of magnitude as compared to the DLS spectrometer. Within the geometrical acceptance the reconstruction efficiency of e^+e^- pairs from ρ/ω amounts to 52%, including matching conditions and additional background rejection methods (see below).

6. 1st and 2nd Level Trigger

A fast trigger is crucial to reduce the interaction rate of $10^6/s$ - the interaction length of the target is 1% - to a tape event rate of $10^2 \cdot 10^3/s$. A Multiplicity/Electron Trigger Array (META) positioned behind the outer MDCs is designed to provide a first level trigger on centrality of the collisions as well as a second level electron trigger in conjunction with the RICH. A time of flight wall consisting of scintillator paddles measures the charged particle multiplicity. This allows a selection of central events due to the impact parameter dependence of the particle multiplicity (Fig. 4) and leads to a reduction of the primary event rate to $10^5/s$. The detector segmentation is chosen to limit the multiple hit probability to values smaller than 0.2.

Using the time of flight information ($\Delta t \sim 400$ ps (FWHM)) for polar angles $> 45^\circ$ a second electron identification is achieved with an efficiency of 96%. At polar angles $< 45^\circ$ a separation of electrons from pions by time of flight is not possible due to the higher momenta. Here, the electron identification is done with a shower detector positioned behind the scintillator paddles. This shower detector consists of a stack of 3 gas detectors and two Pb-layers (two radiation lengths each) in between. Its single lepton efficiency ranges from 80% at an electron momentum of 300 MeV/c to about 90% at 700 MeV/c. Misidentification of background by META results in ≈ 12 electron candidates per collision.

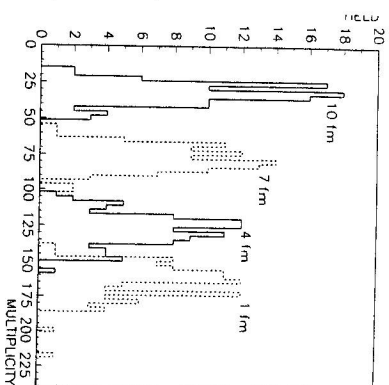


Fig. 4. Charged particle multiplicity distribution on META for different impact parameters. A selection of central events ($b < 2.3$ fm) by multiplicity reduces the interaction rate by a factor of 10.

A fast pattern recognition system allows an online identification of rings in the RICH. These rings are combined with the electron signals given by META to a second level trigger requiring the θ and ϕ correlation of physical tracks. Selecting events with at least two of these candidates reduces the online event rate to the above mentioned tape rate. This second level triggering has to be done within about 100 μs in pipelined steps of 10 μs ; the data remain in the read-out buffers until the trigger decision is made.

7. Signal and Background

After track reconstruction the remaining background consists of uncorrelated e^+ and e^- tracks originating from Dalitz decay processes ($\pi^0 \rightarrow \gamma e^+ e^-$) or external conversions ($\gamma \rightarrow e^+ e^-$). These tracks originate most often from a close pair resulting in only one RICH ring. Both tracks of the pair are detected in the inner MDCs but mostly one of the electrons gets lost by the strong deflection in the field region. Therefore, a powerful rejection method consists in a search for the typical hitpattern of close tracks in the inner MDCs. Rejecting close tracks reduces the background by an order of magnitude to the final amount shown in Fig. 5a.

The different contributions to the reconstructed invariant mass spectrum in Fig. 5a are taken from theoretical models [1][2]. The cross sections are consistent with experimental data [9]. For the ϕ meson the cross section is estimated based on a preliminary calculation [3]. Above 600 MeV/c² the contributions of ρ , ω and ϕ clearly dominate the spectrum. Below 500 MeV/c² the dielectron mass region is dominated by combinatorial background. Fig. 5b shows the reconstructed invariant mass spectrum after subtraction of combinatorial background derived from like sign pairs. The signal from Dalitz decays of Δ 's and η 's as well as from pn-bremsstrahlung is clearly visible below 500 MeV/c². The dotted line shows the residual background resulting from the different spectrometer acceptance for like and unlike sign pairs.

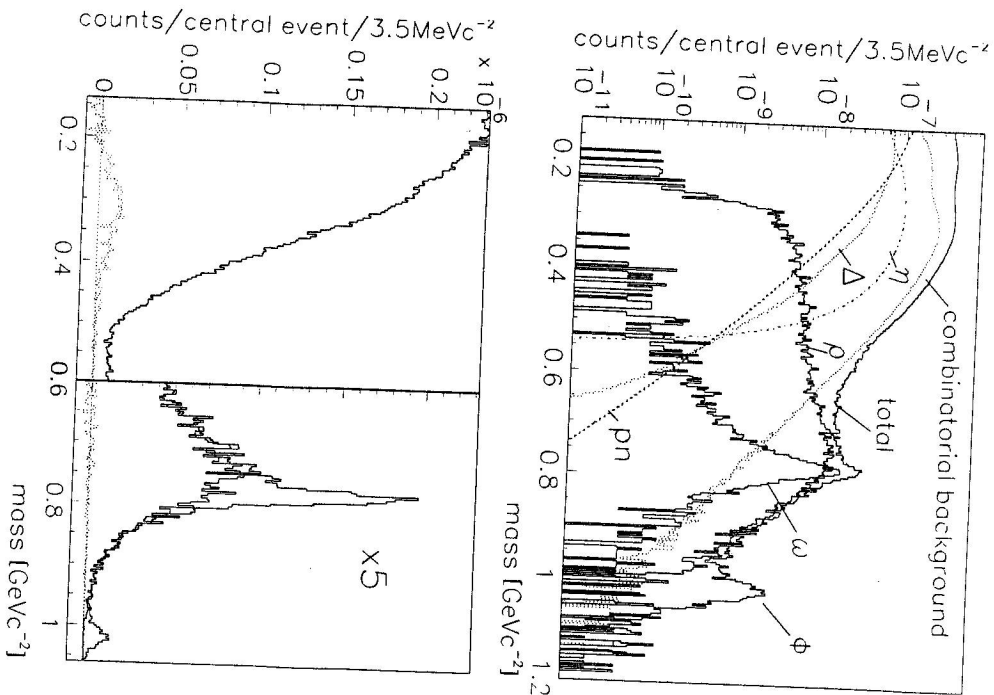


Fig. 5. Invariant mass spectrum for the main e^+e^- sources for 1 AGeV Au+Au collisions. (a) Individual contributions to the total dielectron mass yield. Dalitz decay of η and Δ and pn-bremsstrahlung are the main contributing sources below $0.5 \text{ GeV}/c^2$. Above $0.5 \text{ GeV}/c^2$ of the background obtained from like sign pairs. The remaining background contribution is shown separately (dotted histogram). Note the different scale for masses $> 0.6 \text{ GeV}/c^2$.

8. Conclusions and Prospects

With a high count rate capability and a high geometrical acceptance HADES is able to measure e^+e^- pairs for the heaviest systems at the highest SIS energies. With an invariant mass resolution of better than $1\%(\sigma)$ a clear separation of ω and ϕ from ρ

can be achieved. The reduction of combinatorial background by rejecting close tracks results in a signal to background ratio of 10:1 in the ρ/ω region.

An additional option is the combination of HADES with the photon spectrometer TAPS. This would allow direct measurements of Dalitz decays, in particular of the η meson.

References

- [1] L. Winckelmann, NATO Advanced Study, Bodrum 1993
- [2] Gy. Wolf, W. Cassing and U. Mosel, Nucl.Phys. A552 (1993) 549
- [3] C.-M. Ko, Workshop on Dielectron Production in Relativistic HI Collisions, Darmstadt(GSI) 1994.
- [4] M. Herrmann, B. Frimann and W. Nörenberg, Nucl.Phys A545 (1992) 267
- [5] G. Chanfray and P. Schuck, Nucl.Phys. A489 (1992) 271
- [6] G.E. Brown and M. Rho, Phys.Rev.Lett. 66 (1991) 2720
- [7] T. Hatsuda and S.H. Lee, Phys.Rev. C46 (1992) R34
- [8] M. Asakawa and C.M. Ko, Phys.Rev. C48 (1993) R526
- [9] V. Metag, Prog. Part.Nucl.Phys. 30 (1993) 75
- [10] A. Yegneswaran et al. NIM A290 (1990) 61
- [11] C. Naudet et al. Phys.Rev.Lett. 62 (1989) 2652
- [12] HADES Letter of Intent, Dec 1991, HADES Design Study, Nov 1992
- [13] HADES, GSI Scientific reports 1992 (379-383), 1993